

# Bioprinting with Live Cells

S. Burce Ozler, Can Kucukgul and Bahattin Koc

## 1 Introduction

The loss or failure of an organ or tissue is one of the most devastating, and costly problems in health care. The current treatment methods for organ/tissue loss or failure include transplantation of organs, surgical reconstruction, use of mechanical devices, or supplementation of metabolic products. Due to the growing need for organ transplantation and a lack of donor organs, tissue or organ engineering has progressed as a multidisciplinary field combining life sciences and engineering principles to restore, maintain, or improve function of tissues or organs [1, 2].

Traditionally, tissue engineering strategies are based on the cell seeding into synthetic, biological or composite scaffolds providing a suitable environment for cell attachment, proliferation and differentiation. A scaffold is highly porous complex structure providing an interconnected network that is designed to act as an artificial extracellular matrix (ECM) until the cells form their own ECM. In scaffold-based tissue engineering, three steps must be followed including finding a source of precursor cells from the patient, seeding these cells in vitro into the desired places of scaffold and surgically implanting the scaffold into the patient [3]. Scaffolds have been used to fabricate various tissue grafts including skin, cartilage, bone, blood vessels, bladder and myocardium [4–12]. Bioengineered tissue scaffolds attempt to mimic both the external shape and internal architecture of the replaced tissues.

The modeling of scaffolds has a great impact on the growth and proliferation of cells and a spatially and temporally controlled scaffold design could improve cell growth and differentiation [13]. Although many different scaffold manufacturing techniques such as salt-leaching, porogen melting, gas foaming, electrospinning,

B. Koc (✉) · S. B. Ozler · C. Kucukgul  
Department of Manufacturing and Industrial Engineering,  
Sabanci University, Istanbul, Turkey e-mail:  
bahattinkoc@sabanciuniv.edu

© Springer International Publishing Switzerland 2016

1

K. Turksen (eds.), *Bioprinting in Regenerative Medicine*,  
Stem Cell Biology and Regenerative Medicine, DOI 10.1007/978-3-319-21386-6\_3

25 fiber deposition, molding and freeze-drying have been investigated in the past, it is 26  
challenging to control pore size, porosity, pore interconnectivity and external geom27 etries  
of scaffolds. In recent years, various additive manufacturing based methods 28 such as  
bioplotting, bioprinting, ink-jet printing and stereolithography have been

29 used for biomanufacturing of complex three-dimensional (3D) tissue scaffolds to  
30 overcome the limitations of conventional tissue engineering methods [14]. These 31  
additive manufacturing based techniques allow to fabricate scaffolds layer-by-layer  
32 with controlled external and internal geometries based on computer-aided models  
33 of targeted tissues [15]. Several researchers have investigated designing function34 ally  
gradient porous scaffolds with controllable variational pore size and heteroge35 neous porous  
architecture [16, 17].

36 In scaffold-based tissue engineering, different biomaterials are used for scaffold 37  
fabrication such as porous materials composed of biodegradable polymers (polylac38 tic acid,  
polyglycolic acid, hyaluronic acid and several copolymers), hydroxyapatite 39 or calcium  
phosphate-based materials and soft materials like collagens, fibrin, and 40 various hydrogels.  
Although there is a plenty of choice for scaffold materials, an 41 ideal biomaterial for scaffold  
fabrication should be nontoxic, nonimmunogenic, ca42 pable of maintaining mechanical  
integrity for tissue growth and differentiation with 43 controlled degradation [3].

44 After implantation of a scaffold, it should degrade in a controlled manner and 45 the seeded  
cells should proliferate and migrate into scaffold to replace the scaffold 46 biomaterial.  
Newly-formed extracellular matrix (ECM) fills the places which were  
47 previously occupied by the biomaterial of scaffolds. However, there are some draw48 backs  
to create tissues with biodegradable scaffolds. Mostly, oxygen/nutrient deliv49 ery and  
removal of metabolic waste are insufficient through the micro-channels of 50 a scaffold.  
Additionally, biodegradation of the scaffold induces inflammation. Even 51 though the  
biomaterials used may not be directly toxic, they can be metabolized to 52 toxic byproducts  
[18].

53 Because of the above mentioned drawbacks, the recent tissue engineering studies 54 tend  
towards ‘scaffold-free’ techniques. During the embryonic maturation, tissues 55 and organs  
are formed without the need for any scaffolds [19, 20]. The self-assem56 bly and self-  
organizing capabilities of cells and tissues are main driver for the field 57 of scaffold-free  
tissue engineering. Self-assembly based tissue engineering aims to 58 produce fully biological  
tissues with specific compositions and shapes having the 59 ability to grow their own ECM,  
and therefore to reduce the immunogenic reactions 60 and other unpredicted complications  
based on the use of scaffolds [21].

61 One way of implementing the self-assembly approach is the cell sheet technol62 ogy, which  
has been applied clinically for the repair of skin, cornea, blood vessels, 63 and cardiomyocyte  
patches to repair partial heart infarcts [18, 22, 23]. Another self64 assembly-based approach

is founded on the recognition that ‘nature knows best’. This approach relies on the principle that cell aggregates can be used as building blocks, since they have the intrinsic capacity to fuse together, known as tissue fluidity and self-assemble through morphogenetic processes if they are deposited in

close spatial organization [24–26]. The engineering of 3D living structures supported by the self-assembly and self-organizing capabilities of cells is commonly termed ‘bioprinting’. Bioprinting is an extension of tissue engineering, where the cells are delivered through the application of additive manufacturing techniques [27, 28]

This chapter focuses on scaffold-free tissue engineering and its adaptation to the technology of three dimensional bioprinting. Further, the importance as well as the challenges for 3D bioprinting using stem cells will be discussed in this chapter.

## 2 Bioprinting with Live Cells

### 2.1 2D Patterning and Cell-Sheet Technology

Placing cells into special patterns using the laser light has been one of the first methods used for 2D cell patterning [14]. These laser-based techniques utilize transparent ribbons on which one side is coated with cells that are either adhered to a biological polymer through initial cellular attachment or uniformly suspended in a thin layer of liquid or a hydrogel. A pulsed laser beam is transmitted through the ribbon and is used to push cells from the ribbon to the receiving substrate which is coated with hydrogels.

While laser based approaches enable to pattern living cells on a substrate and to layer multiple cell types, laser-based techniques have been also explored for positioning of cells in microarrays [32]. The resolution of laser-assisted bioprinting is affected by different factors such as the laser fluence, the wettability of the substrate, and the thickness and the viscosity of the biological layer [33]. Guilot and his group studied the effect of the viscosity of the bioink, laser energy, and laser printing speed on the resolution of cell printing [34] as shown in Fig. 1.

By using this method, various cell types including human osteosarcoma, rat cardiac cells and human umbilical vein endothelial cells (HUVEC) could be printed with micrometer accuracy on Matrigel as the absorptive layer [31, 35, 36]. More recently, the biological laser printing was used to print sodium alginate, nano-sized hydroxyapatite (HA) and human endothelial cells [37]. However, most of these methods are limited to two-dimensional patterning and it is difficult to fabricate three-dimensional tissue constructs because of process-induced cell injury. The thermal stress and ultraviolet radiation caused by laser printing could also affect

the cell viability.

105

Similar to 2D patterning, cell sheet technology is another scaffold-free method for construction of 2D and 3D engineered tissues. In this method, cells can be moved from a culture dish as a relatively stable confluent monolayer sheet without destroying cell-cell contacts. In order to build a substantial 3D tissue volume, many sheets need to be culminated in high amount of cells which requires vascularization for cell viability [15].

L'Heureux and his group produced a tissue engineered blood vessel using a cell sheet approach based on cultured human cells. The developed vessel contained all three histological layers such as the endothelium, the media and the adventitia. In

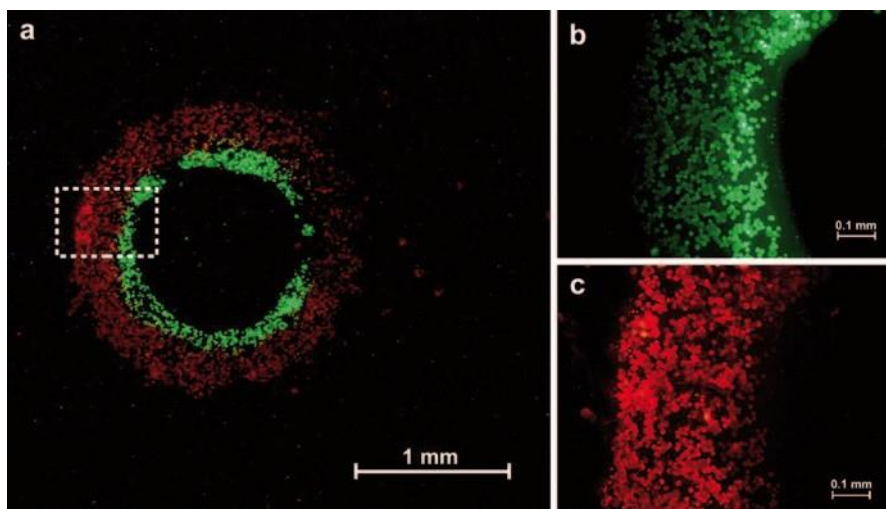


**Fig. 1** Laser-assisted sequential two color cell printing in 2D. **a** The two cell suspensions (6·10<sup>7</sup> cells/ml in DMEM, supplemented with 1% (w/v) alginate) were then printed according to a pattern of concentric circles). **b** Green Calcein stained cells within the region of interest as defined in **1a** (dashed rectangle). **c** Red fluorescent Dil-LDL stained cells within the same region of interest. (Adapted from [34])

<sup>114</sup> this self-assembly approach, smooth-muscle cells and fibroblasts were cultured in <sup>115</sup> medium containing serum and ascorbic acid and produced their own extracellular <sup>116</sup> matrix (ECM). The smooth-muscle cell sheet was placed around a tubular mandrel <sup>117</sup> to produce the media of the vessel. A similar fibroblast cell sheet was wrapped <sup>118</sup> around the media to provide the adventitia after 8 weeks of maturation. Finally, <sup>119</sup> the tubular support was removed and endothelial cells were seeded in the lumen <sup>120</sup> to form the endothelium. The tissue engineered blood vessel has burst strength of <sup>121</sup> over 2500 mm Hg which is significantly higher than that of human saphenous veins <sup>122</sup> (1680 ± 307 mm Hg) [23]. Sheet-based tissue engineering has been used by the same <sup>123</sup> group to produce tissue engineered blood vessel (TEBV) suitable for autologous <sup>124</sup> small diameter arterial revascularization in adult patients. Fibroblasts were cultured <sup>125</sup> in conditions promoting

extracellular matrix (ECM) deposition to produce a cohesive sheet that can be detached from the culture flask. This approach also eliminates the use of smooth-muscle cells, whose early senescence is related with decreased burst pressures in human models. The decellularized internal membrane (IM) and living adventitia were assembled by wrapping fibroblast sheets around a temporary Teflon coated stainless steel support tube. After weeks-long maturation and dehydration to form an acellular substrate, the steel tube was removed and endothelial cells were seeded in the lumen of living TEHV. The transplantation of these blood vessels into dogs demonstrated good handling, suturability by the use of conventional surgical techniques. Ultimately, this is an effective approach to produce a completely biological and clinically applicable TEHV in spite of its relatively long production time ( $\approx 28$  weeks) which clearly prevents its urgent clinical use [22].

Okano and colleagues have engineered a long-lasting cardiac tissue based on a similar self-assembled sheet based approach. In their method, culture dishes are first coated with a temperature-responsive polymer, poly (N-isopropylacrylamide)

(PIPAAm). The surface is relatively hydrophobic at  $37^\circ\text{C}$  allowing cells to attach and proliferate, while cooling below  $32^\circ\text{C}$  (typically  $20^\circ\text{C}$  for 30 min) makes the surface hydrophilic and causes the cells to detach without the use of enzyme digestion reagent. When grafted PIPAAm layer thickness is between 15 and 20 nm, temperature-dependent cell adhesion and detachment can be observed. Once the cells spread and confluent on the surface, they can be spontaneously detached as a contiguous cell sheet by reducing the temperature. This process does not disrupt the cell-cell junctions because no enzymes like trypsin are required. Additionally, basal surface extracellular matrix (ECM) proteins such as fibronectin are preserved after detachment which enables easy attachment of cell sheets to host tissues and even wound sites with minimal cell loss. In order to obtain tissue constructs with characteristic physiological cellular functions *in vitro*, heterotypic cell-cell interactions are inevitable. As shown in Fig. 2, it is possible to modify the above-mentioned technique in order to develop patterned cell sheets using two or more kinds of cell source. Domains on petri dishes were grafted by using area-selective electron beam polymerization of PIPAAm. After cells were cultured on the patterned surfaces at  $37^\circ\text{C}$ , the temperature was decreased to  $20^\circ\text{C}$ . Cells on the PIPAAm surface are detached where other cell types were seeded subsequently by increasing the temperature to  $37^\circ\text{C}$ . Therefore, two cell types can be co-cultured in desired places which improve cellular functions [18, 38, 39]. Three-dimensional myocardial tubes

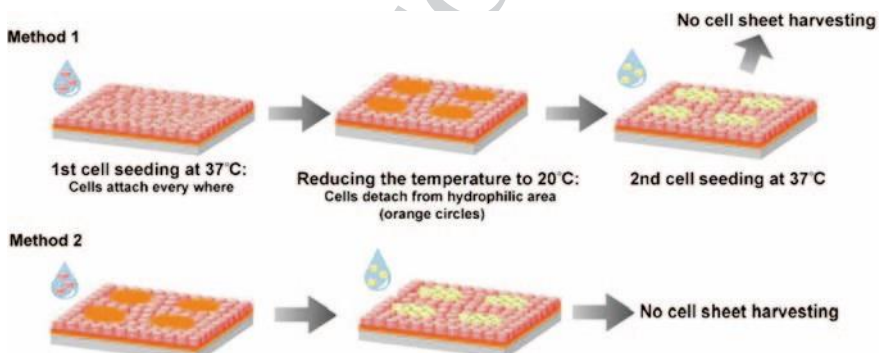


**Fig. 2** Schematic diagram of methods of cell seeding for patterned co-culture on PIPAAm-grafted surfaces. (Adapted from [40])

159 were fabricated using neonatal rat cardiomyocyte sheets cultured on temperature 160 responsive culture dishes [40, 41]. Due to the functional gap junction formation, 161 electrical coupling of cardiomyocyte sheets was obtained quickly and the construct 162 was implanted [42]. Four weeks after the implantation, the myocardial tubes were 163 integrated with the host tissues showing spontaneous and synchronized pulsation 164 [38, 43]. Using this versatile method, functional and transplantable tissue sheets are 165 produced from different cell types including epidermal keratinocytes [44], kidney 166 epithelial cells [45] and periodontal ligaments [46, 47].

167 Two-dimensional cell patterning or cell-sheet based approaches have been suc-  
168 cessful tissue engineering approaches. However, the engineered constructs  
fabricated with these methods are limited to 2D cell patterns or simple shapes  
because 170 of the flat and uncontrolled shape of the cell sheets. In addition, many  
sheets also 171 need to be culminated in high amount of cells which requires pre-  
vascularization 172 of the sheets for 3D tissue constructs. Therefore, several  
bioprinting approaches 173 have been developed for fabricating 3D tissue  
constructs with live cells. Two major 174 approaches, ink-jet based and extrusion  
based 3D bioprinting methods will be ex175 plained in details below.

176

177

## 178 **2.2 Inkjet-Based Bioprinting**

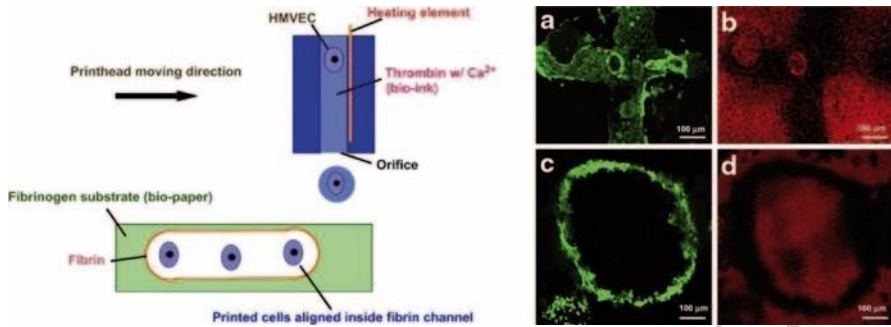
179

180 In inkjet-based bioprinting, a bioink made of cells and biomaterials are printed in 181 the form of droplets through cartridges onto a substrate. There are two types of 182 inkjet printing including continuous inkjet printing (CIJ) and drop-on-demand ink 183 jet printing (DOD). In CIJ mode, a jet is obtained by forcing the liquid through an 184 orifice under an external pressure and it breaks up into a stream of droplets. In DOD 185 mode, a pressure pulse is applied into the fluid which generates drops only when 186 needed. For ink-jet printing of cells, there are two most commonly used approaches: 187 thermal and piezo-electric inkjet printing. For thermal inkjet printing, small vol 188 umes of the printing fluid are vaporized by a micro-heater to create the pulse that 189 expels droplets from the print head. In piezoelectric inkjet printing, a direct me 190 chanical pulse is applied to the fluid in the nozzle by a piezoelectric actuator, which 191 causes a shock wave that forces the bioink through the nozzle [48]. However, there 192 have been only a few examples of cell deposition by piezoelectric ink-jet printing 193 due to the electrically conducting ink formulations and contamination concerns on 194 ink recycling [24].

195 Inkjet-based bioprinting (Fig. 3) enables to deposit different cell types in precise 196 orientations relative to the print surface and to each other at micrometer resolution 197 by

controlling the ejection nozzles and timing of spray [49]. Wilson and Boland first<sup>198</sup> adapted the ink-jet printers for the manufacture of cell and protein arrays, which<sup>199</sup> have the advantage of being fully automated and computer controlled [50]. In their<sup>200</sup> next study, cell aggregates were printed onto thermosensitive gels layer-by-layer<sup>201</sup> in order to demonstrate the fusion between the closely-placed cell aggregates [51].

202 The same group deposited CHO cells and rat embryonic motoneurons as an ‘ink’



**AQ1** Fig. 3 Schematic diagram of inkjet bioprinting methods of cells with fibrin channel scaffold printed microvasculature. **a** Printed perpendicular microvasculature cultured for 14 days. **b** Integrity of the printed structure stained using Texas Red conjugated dextran molecules of 3000 MW. **c** Printed ring shaped microvasculature cultured for 21 days. **d** Integrity of printed structure cultured for 21 days

203 onto several ‘bio-papers’ made from soy agar and collagen gel. They demonstrated  
204 also that the mammalian cells can be effectively delivered by a modified thermal  
205 inkjet printer onto biological substrates and that they retain their ability to function  
206

[52]. Cui and Boland used also thermal inkjet printing to produce cell containing  
207 fibrin channels by printing human microvascular endothelial cells onto thin layers  
208 of fibrinogen as shown in Fig. 3. During the incubation period, the cells proliferated  
209 and formed branched tubular structures mimicking simple vasculature [53].  
210

Inkjet bioprinting has been progressed to fabricate 3D biological structures by  
211 the use of readily crosslinked hydrogels such as alginate. In published studies, cells  
212 have been mixed with alginate solutions and crosslinked with calcium chloride to  
213 create cell encapsulating hydrogels having defined 3D structures [54–56]. In a more  
214 recent study, alginate has been used as a constituent of bioink and it was mixed with  
215

NIH 3T3 mouse fibroblasts cell suspension in order to fabricate zigzag cellular  
216 tubes with an overhang structure using a platform-assisted 3D inkjet  
bioprinting

217 system [57].

218

219 Although inkjet bioprinting has been one of the most commonly used method  
220 in printing living cells and biomaterials, cell aggregation, sedimentation and cell-  
221 damage because of the high shear stresses are common drawbacks of this method.

222

223 Cell aggregation and sedimentation may be prevented by frequent stirring of the  
224 cell mixture, which can result in reduced cell viability if the cells are sensitive to the  
225 shear forces [58]. Another problem limiting the inkjet bioprinting is the clogging  
226 of the nozzle orifice. Low viscosity surfactants can be added to the ink which can  
cause additional challenges such as cell damage [59].

227

228 Recently, two research groups successfully address the sedimentation and cell  
229 aggregation problem during the inkjet bioprinting. Chahal and coworkers used a  
230 surfactant (Ficoll PM400) create neutrally buoyant MCF-7 breast cancer cell sus-  
pensions, which were ejected using a piezoelectric drop-on-demand inkjet printing

231

232 system. They demonstrated that Ficoll PM400 did not have adverse effects on cell  
233 viability. Moreover, neutrally buoyant suspension greatly increased the reproducibility  
of consistent cell counts, and eliminated nozzle clogging. [60].

234 Ferris et al. used two different commercially available drop-on-demand printing  
235 systems in order to reproducibly print several different cell types over long printing  
236 periods. The bio-ink based on a novel microgel suspension in a surfactant-containing  
237 tissue culture medium can prevent the settling and aggregation of cells, while meeting the  
238 stringent fluid property requirements needed for many-nozzle commercial inkjet print  
heads. They could print two cells types simultaneously from two different inkjet print  
heads, which is a innovative way to biofabricate more complex multi-cellular structures  
[61].

241

242

### 243 **2.3 Self-Assembly Based Bioprinting**

244

245 The autonomous organization of components from an initial state into a final pattern  
246 or structure without external intervention is called self-assembly. The aim of the

247 self-assembly-based bioprinting is the use of the inherent organizational capacity of  
248 cells into tissues and eventually organs by mimicking natural morphogenesis. The

249 best examples of tissue self-organization and self-assembly are in the field of devel-  
250 opmental biology and scaffold-free biomimetic approach has deep roots in devel-  
opmental biology [20]. Malcolm Steinberg published papers, in which he  
formulated fundamental thermodynamic rules determining tissue self-assembly  
and developed



<sup>253</sup> differential adhesion hypothesis (DAH) explaining the fluidic nature of cell sorting <sup>254</sup> and tissue self-assembly [62–64]. Therefore, the novel scaffold-free biomimetic tis<sup>255</sup> sue engineering paradigm relies on the principle that in vitro tissue assembly from <sup>256</sup> single cells or tissue aggregates is feasible.

<sup>257</sup> Based on the self-assembly principle, it is possible to fabricate reliable and re<sup>258</sup> producible 3D tissue constructs having defined topology and functionality in vitro <sup>259</sup> when combined with bioprinting techniques. The disadvantage of this method is

<sup>260</sup> that the development of the natural ECM is time consuming and in vitro self-as<sup>261</sup> sembly may vary with fully physiological conditions. The bioprinting of 3D tissue

<sup>262</sup> constructs is achieved via a three-phase process: (1) preprocessing or bio-ink prepa<sup>263</sup> ration; (2) processing, i.e. the actual automated deliver/printing of the bio-ink parti<sup>264</sup> cles into the bio-paper by the bioprinter; and (3) postprocessing, i.e. the maturation/

<sup>265</sup> incubation of the printed construct in the bioreactor [19]. Self-assembly occurs in an <sup>266</sup> *in vivo* like, fully controllable cell environment (bioreactor) by the differentiation of <sup>267</sup> cells at the right time, in the right place and into the right phenotype and eventually <sup>268</sup> the assembly of them to form functional tissues. Based on this approach, a perfusion <sup>269</sup> reactor is used for the maturation of a bioprinted macrovascular network in order

<sup>270</sup> to obtain the required mechanical properties. Microvascular units consisting of cy<sup>271</sup> lindrical or spherical multicellular aggregates were fabricated by the parenchymal <sup>272</sup> and endothelial cells. Afterwards, microvascular units were located in the macro<sup>273</sup> vascular network for the perfusion supporting self-assembly and the connection to

<sup>274</sup> the existing network. Multicellular spherical and cylindrical aggregates have been

<sup>275</sup>

<sup>276</sup>

<sup>277</sup>

<sup>278</sup>

<sup>279</sup>

<sup>280</sup>

<sup>281</sup>

<sup>282</sup>

<sup>283</sup>

<sup>284</sup>

<sup>285</sup>

<sup>286</sup>

<sup>287</sup>

<sup>288</sup>

<sup>289</sup>

<sup>290</sup>

<sup>291</sup>

<sup>292</sup>

constructed by using 3D printing methods, which enable to achieve flexibility in tube diameter and wall thickness and to form branched tubular structures. However, the printed cell aggregates should be perfectly supported by hydrogels for 3D printing [21]. Forgacs and his group employed this novel technology to print cellular topologically defined structures of various shapes. Cardiac constructs were built using embryonic cardiac and endothelial cells and their postprinting self-assembly resulted in synchronously beating solid tissue blocks, where the endothelial cells were organized into vessel-like conduits [65]. In their more recent study, the same group utilized the self-assembly approach in order to bioprint small-diameter, multi-layered, tubular vascular and nerve grafts using bio-ink composed of aortic smooth muscle cells (HASMC), human aortic endothelial cells (HAEC), human dermal fibroblasts (HDFb) and bone marrow stem cells (BMSC), respectively as shown in Fig. 4 [25]. Similarly, in another study, self-assembled cell-based microtissue blocks were used to generate small diameter tissue-engineered living blood vessels (TEBV). Microtissues composed of human-artery-derived fibroblasts (HAFs) and endothelial cells (HUVECs) were cultured for 7 and 14 day under pulsatile flow/mechanical stimulation in a designed bioreactor or static culture conditions with a diameter of 3 mm and a wall thickness of 1 mm. Self-assembled microtissues

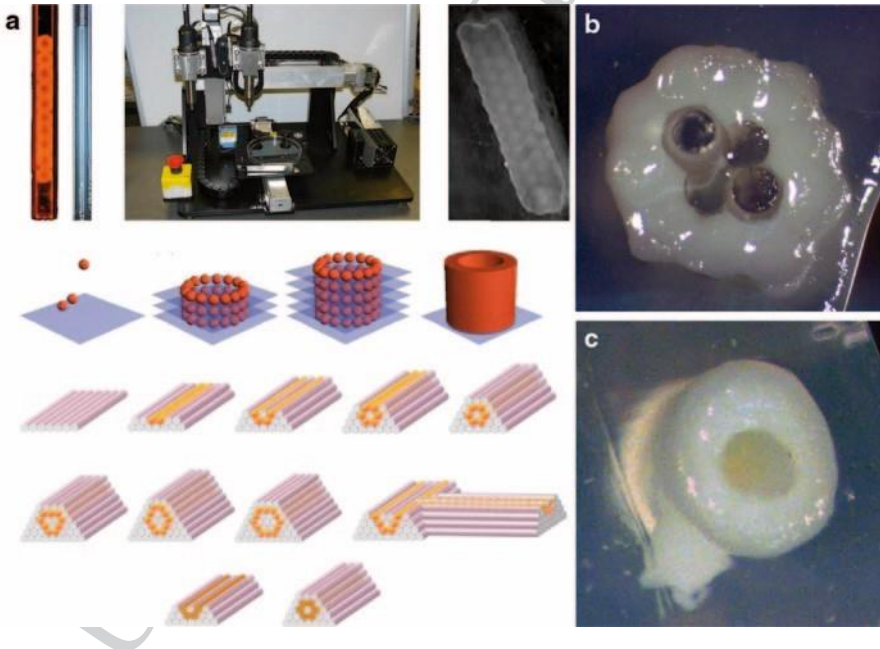


**Fig. 4** **a** Organovo bioprinter with cell and hydrogel printing heads and schematics to print tubular structures with cellular spheroids: layer-by-layer deposition of spheroids into the hydrogel. **b** Cross-section of a vascular graft printed with four central rods 12 h post-printing. All cellular cylinders have fused to form a continuous conduit. **c** A vascular construct (ID =600 μm) at 14 days post-perfusion. (Adapted from [25])



**Fig. 5** Bioprinting of aortic valve conduit. **a** Aortic valve model reconstructed from micro-CT images. The root and leaflet regions were identified with intensity thresholds and rendered separately into 3D geometries into STL format (*green* color indicates valve root and *red* color indicates valve leaflets); **b**, **c** schematic illustration of the bioprinting process with dual cell types and dual syringes; **b** root region of first layer generated by hydrogel with SMC; **c** leaflet region of first layer generated by hydrogel with VIC; **d** fluorescent image of first printed two layers of aortic valve conduit; SMC for valve root were labeled by cell tracker *green* and VIC for valve leaflet were labeled by cell tracker *red*. **e** as-printed aortic valve conduit. (Reproduced with permission [75]).

293 composed of fibroblasts showed accelerated ECM formation and a layered tissue **AQ2**  
 formation was obtained only in flow/mechanical stimulation conditions [66] Fig. 5. ■

295 An alternative approach for multicellular spheroid assembly technique for bio296  
 fabrication was developed by Nakayama and his group. In their technique, they 297 used a so  
 called needle-array system instead of using a bioprinter. A robotic system 298 was developed  
 in order to skewer the multicellular spheroids into medical-grade

299 stainless needles, which served as temporal fixators until multicellular spheroids 300 fused  
 each other. They could fabricate complex 3D scaffold-free cell constructs 301 with different  
 types of cells including chondrocyte, hepatocyte, cardiomyocyte and 302 vascular smooth  
 muscle cell. One of the advantages of this technique is the easy 303 removal of the temporary  
 supports without contamination with exogenous materi-  
 304 als [3].

305 Apart from the above mentioned applications, a new method is presented to rap306  
 idly self-assemble cells into 3D tissue rings without the use of additional equip307  
 ment. This method enables fabrication of engineered tissue constructs entirely from  
 308 cells by seeding cells into custom made annular agarose wells with 2, 4 or 6 mm  
 309 inside diameters. Different cell types including rat aortic smooth muscle cells  
 and

310 human smooth muscle cells are used with varying seeding conditions and culture  
 length to form tissue rings. The strength and modulus of tissue rings increased with  
 311 ring size and decreased with culture duration. Rat smooth muscle cell rings with  
 an 312 inner diameter of 2 mm are cohesive enough for handling after 8 days  
 incubation 313 and they yield at 169 kPa ultimate tensile strength. Furthermore, it  
 is also pos314 sible to fabricate tissue tubes by transferring the rings onto silicone  
 tubes, sliding 315 them into contact with one another and incubating them for an  
 additional 7 days. 316 Although these rings are not as strong as ring segments of  
 native blood vessels or 317 TEBV fabricated from cell sheets for 2–3 months, the  
 presented method allows de318 veloping 3D tissue constructs from aggregated cells  
 within an experimentally useful <sup>319</sup> time frame (1–2 weeks) [67]. Likewise created  
 smooth muscle cell tissue rings and 320 rings fabricated from cells seeded in fibrin  
 or collagen gels are compared based on 321 their relative strength and utility for  
 tissue engineering. All tissue rings were cul322 tured for 7 days in supplemented  
 growth medium which includes  $\epsilon$ -amino caproic

323 acid, ascorbic acid, and insulin-transferrin-selenium. Ultimate tensile strength and 324  
 stiffness values of tissue rings were two-fold higher than fibrin gel and collagen gel 325

rings. Tissue rings cultured in supplemented growth medium exhibit a three-fold increase in tensile strength and stiffness in comparison to the tissue rings cultured in standard growth medium [68].

The approach of using microtissues as building blocks to form larger structures is further used by other research groups in order to investigate the capacity of cell aggregates. After a preculture period for 7 days of HUVEC spheroids, they were mixed with NHF cells and were able to reassemble and form microtissues

with the NHF cells on the inside and coated with HUVEC on the outside [69]. Additionally, the kinetics of the cellular self-assembly also differs from one cell type to the other. While H35 cells formed relatively stable rod structures inside the recesses of micromolded agarose gels, NHF cells reassembled quickly the initial rod structures to a final spheroid structure [70].

337

338

## 2.4 Extrusion-Based Bioprinting

339

340

341

Bioprinting methods based on extrusion of cell or cell-laden biomaterials use self-assembly cells to construct 3D biological constructs. The main principle of extrusion-based bioprinting techniques is to force continuous filaments of materials including hydrogels, biocompatible copolymers and living cells through a nozzle with a help of a computer to construct a 3D structure [27]. Extrusion-based printers usually have a temperature-controlled material handling and dispensing system and stage with the movement capability along the x, y and z axes. The printers are directed by the CAD-CAM software and continuous filaments are deposited in two dimensions layer-by-layer to form 3D tissue constructs. The stage or the extrusion head is moved along the z axis, and the printed layers serve as a base and support for the next layer. Pneumatic or mechanical (piston or screw) are the most common techniques to print biological materials for 3D bioprinting applications [33]. Additionally, novel multi-nozzle biopolymer deposition systems were developed for freeform fabrication of biopolymer-based tissue scaffolds and cell-embedded tissue

constructs [71, 72].

An extrusion-based printer was used to deposit living cells by Williams and co-workers.

Instead of using a thermally crosslinked biomaterial, which can flow

at room temperature, but crosslink into a stable material at body temperature, they used

Pluronic F-127 and type I collagen to encapsulate human fibroblasts and bovine aortic endothelial cells (BAECs) separately. These materials flow at physiologically suitable

temperatures (35–40°), but crosslink at room temperature. They demonstrated the availability of CAD/CAM technology to fabricate anatomically correct shaped constructs

and also examined several environmental factors with respect to the viability of the extruded cells [73, 74]. Recently, different research groups used the similar extrusion

systems in order to fabricate anatomically accurate and mechanically heterogeneous aortic valves as shown in Fig. 1 [75, 76].

Several groups used high resolution extrusion systems to print different type of cells encapsulated in various hydrogels. For instance, Chang et al. printed HepG2

cell encapsulated sodium alginate through a pneumatically powered nozzle and examined the process parameters, the dispensing pressure and the nozzle diameter, regarding the cell viability and recovery [77]. In another study, alginate hydrogel was used with calcium sulfate as a crosslinking agent to fabricate pre-seeded plants of arbitrary geometries and the printed constructs showed high viabilities [78]. Although the cell viability after printing is important, it is also important that the cells perform their essential functions in the tissue constructs.

Extrusion-based printing allows the construction of organized structures within a realistic time frame, and hence it is the most promising bioprinting technology.

The main advantage of extrusion-based bioprinting is the ability to print very high cell densities. Some groups developed 3D bioprinters in order to use multicellular spheroids or cylinders as bioink to create 3D tissue constructs [19, 21, 25, 79–81]. However, preparing bioink requires time-consuming manual operation and makes totally automated and computer-controlled 3D bioprinting impossible in earlier

studies. Therefore, our group focused on the development of a continuous printing approach in order to extrude cylindrical multicellular aggregates using an extrusion-based bioprinter, which is an automated, flexible platform designed to fabricate 3D tissue engineered cell constructs. In order to bioprint anatomically correct tissue constructs directly from medical images, the targeted tissue or organ must be biomodeled. In the following section, the details of modeling and developing path planning for automated direct cell bioprinting will be explained.

392

393

#### 2.4.1 Biomodeling

394

395

In order to obtain an anatomically accurate tissue constructs, several imaging methods for data acquisition of tissue organ such computed tomography (CT) and magnetic resonance imaging (MRI) could be used. The obtained medical images are then transferred to a special segmentation software, where the images are represented with stack of numerous planar scan captures (Fig. 6a). The segmented 3D

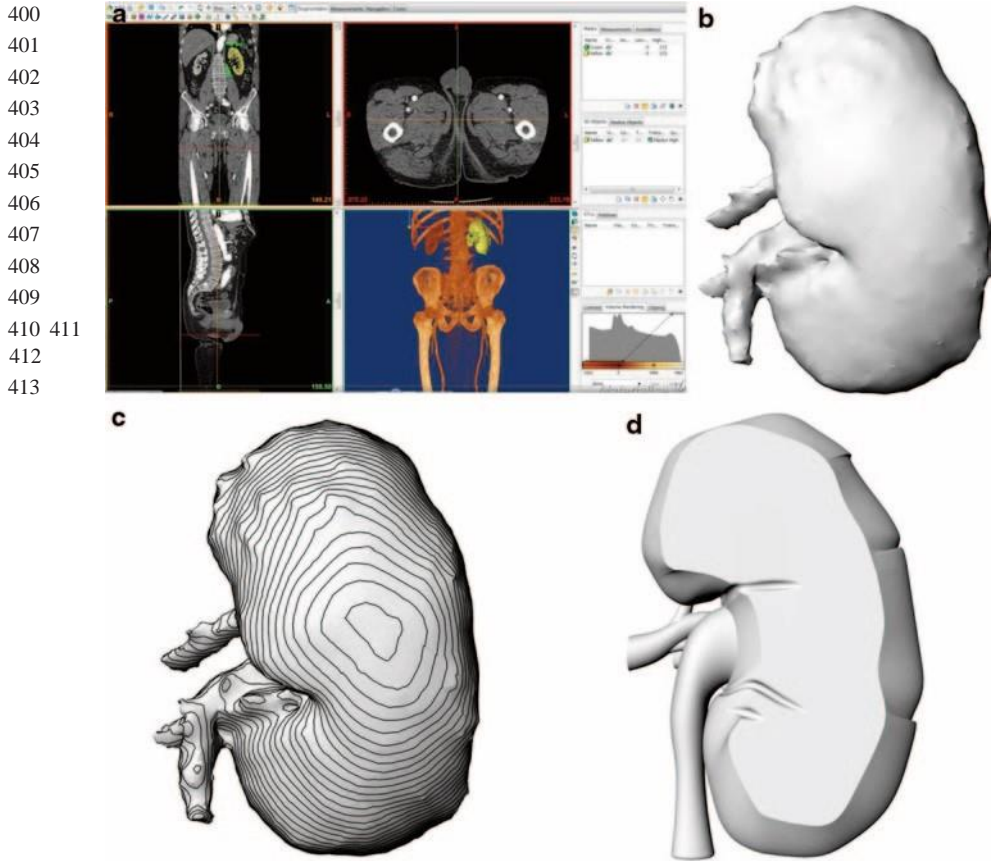


**Fig. 6** Biomodeling of the bioprinted tissue/organ **a** segmentation of the targeted tissue/organ **b** mesh model of segmented model **c** slicing of CAD model

surface geometry is transformed to a CAD model which is a mesh model of the object (Fig. 6b). In order to generate bioprinting path planning as well as the topology optimization for bioprinting processes, the resultant mesh models need to be represented by smooth parametric surfaces. The mesh model is then sliced with consecutive planar cross-sections, resulting in closed contour curves for each thin layer slice [28] (Fig. 6c). Those contour curves are basically the surface boundaries of tissue constructs. Obtained contour curves need to smoothed by B-spline curve fitting from their control points, in order to generate smooth parametric surfaces and finer surface geometry (Fig. 6d). The resultant CAD model is then ready to be used for path planning and topology optimization purposes for biomimetic 3D bioprinting.

Recently, novel computer-aided algorithms and strategies are developed to model and 3D bioprint a scaffold-free human aortic tissue construct biomimetically by our group. Medical images obtained from magnetic resonance imaging (MRI) are used



**Fig. 7** Biomimetic modeling of aorta directly from medical images **a** segmentation from medical images **b** Conversion to a CAD model

414 to obtain the geometric and topological information of the targeted aorta. In order to 415  
 obtain 3D computer models of the aortic tissue, MRI images are segmented using a 416  
 segmentation software and converted into CAD model (Fig. 7). For tool path plan<sup>417</sup> ning as  
 well as for optimization of 3D bioprinting, the resultant mesh model of aorta<sup>418</sup> converted  
 to a CAD model with smooth parametric surfaces. Three-dimensional<sup>419</sup> bioprinting path  
 planning and parameter optimization are then developed. The de<sup>420</sup> veloped self-supporting  
 methodology is used to calculate corresponding tool paths<sup>421</sup> for both cell aggregates and  
 the support structures, which control the bioprinter for<sup>422</sup> 3D printing of a biomimetic aortic  
 construct [74].

423  
 424

#### 425 **2.4.2 Path Planning and Optimization for Bioprinting** 426

427 In order to bioprint an anatomically correct tissue constructs with live cells layer-by<sup>428</sup>  
 layer, the generated computer model of this construct needs to be sliced by planar  
 429 cross-sections, resulting in closed contour curves for each layer. Then those layers<sup>430</sup>  
 need to be filled by appropriate types of cellular aggregates with supportive hydro<sup>431</sup> gel  
 walls surrounding them for keeping the biomimetic form. In our recent work,<sup>432</sup>  
 multicellular cell aggregates are 3D bioprinted based on computer-aided continuous<sup>433</sup> and,  
 interconnected tool-path planning methodologies. Continuous bioprinting en<sup>434</sup> ables to  
 design and 3D bioprint extruded multicellular aggregates according to the  
 435 computer model of the targeted tissue. The Zig-zag and Contour Offsetting pattern<sup>436</sup>  
 tool-path methodologies are developed to 3D bioprint different shaped structures<sup>437</sup> with  
 multiple layers. A CAD software package was used for developing algorithms<sup>438</sup> for  
 continuous and connected bioprinting path plans. In order to keep the 3D forms<sup>439</sup> of printed  
 structures during the maturation period, a biocompatible and bio-inert  
 440 agarose-based hydrogel was used as a support material [75]. The developed bio<sup>441</sup>  
 printing process starts from the bottom layer and follows the generated path plan for<sup>442</sup> each  
 particular layer consecutively through the top layer. At a layer, support mate<sup>443</sup> rial enclosing  
 the cellular aggregates are printed first, and then cellular aggregates<sup>444</sup> are deposited to fill  
 the respective contour areas.

445 In Fig. 8, schematic view of pat planning strategies are showed for a layer. Figure  
 8a-b shows Zig-zag whereas Fig. 8c-d shows Contour Offsetting path planning.

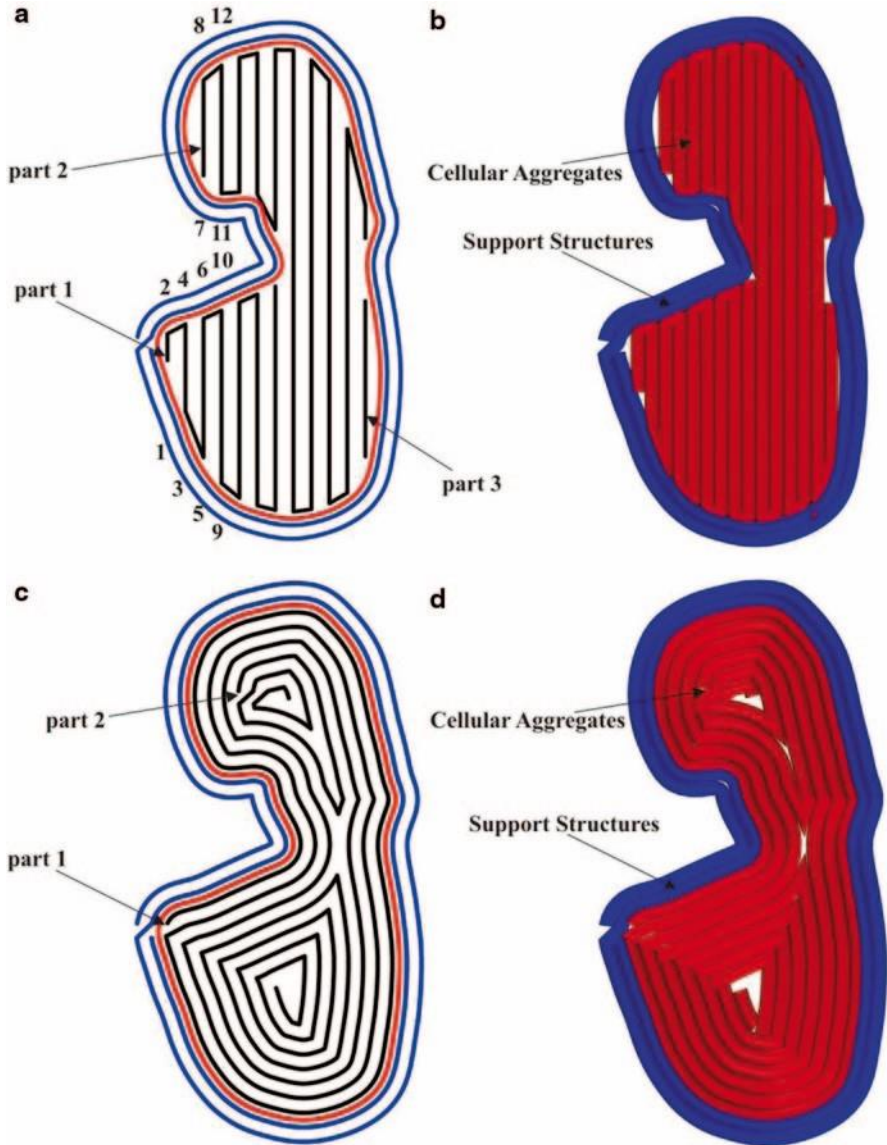


**Fig. 8** Path planning for bioprinting a–b Zig-zag pattern c–d Contour offsetting path planning

In both Zig-zag and Contour Offsetting patterns, outer supportive hydrogel walls' 447 tool path are generated with offsetting the contour curve with a deposited cellular 448 or hydrogel extrusion diameter. Placement of support structures before the cellular 449 aggregates provides necessary conditions for cell fusion and structure conservation. 450 In Zig-zag pattern path planning strategy, contour curves are



crossed with parallel consecutive lines, each separated by extrusion diameter, and an intersection point is generated for each cross as shown in Fig. 8a. Zig-zag pattern path planning strategy aims to fill the contour area by following a zig-zag patterned path way between the generated intersection points as uninterrupted as possible.

In Contour Offsetting path plan strategy, cellular aggregates' path plan is formed by offsetting the contour curve to fill the entire area. After the necessary amount of offset curves is generated, they are joined by small line segments to enable continuous bioprinting. That strategy also aims to fill the contour area with minimum number of cellular aggregate as shown in Fig. 8c).

After the path plan is calculated, the coordinates of these movements are transferred to bioprinter to guide the deposition path plan in order to obtain anatomically correct tissue constructs. In Fig. 8b and Fig. 8d, the finalized generated path plans of cellular aggregates (red) and support structures (blue) are shown for both path planning strategies.

465

466

### 467 2.4.3 Continuous Cell Printing

468

In our recent work, a novel bioprinting method is used for precise deposition of multicellular aggregates composed of different combinations of mouse aortic smooth muscle cells (MOVAS), NIH 3T3 mouse fibroblast cells, human umbilical vein endothelial cells (HUVEC), and human dermal fibroblast (HDF) cells according to computer-generated paths as shown in Fig. 9 [83]. The proposed methodology increases the contact of cylindrical multicellular aggregates in adjacent bioprinted layers, facilitates the fusion of cells and accelerates the maturation process. More significantly, this procedure reduces the human intervention at forming of cylindrical multicellular aggregates and therefore, increases the reproducibility.

The printed 3D multicellular structures are examined for their mechanical strength, shape deformation with time, cell viability and cell fusion. The printed constructs having different shapes deformed during the incubation period (up to

10-days) and generally a shrinking between 20 – 38 % was observed. After 4 or 7 days incubation, the support structures of well-defined and random-shaped printed structures composed of MOVAS, HUVEC and NIH 3T3 multicellular aggregates were manually removed and the fused cell structures could be transferred with forceps into a falcon filled with PBS (Fig. 10a). It is remarkable that the stripe shaped constructs composed of HUVEC/HDF cell aggregates had a small deformation percentage (85 % after 3-days incubation) and were sufficiently sturdy to be handled and transferred as shown in Fig. 10b.[83]. MOVAS/HUVEC/NIH 3T3 multicellular aggregates fused within 3 days, which corresponds to earlier studies [25, 81]. The cell viability upon implementation was high (97 %) showing that the cellular bioink preparation method is successful in comparison to other studies in literature. It

seems that multicellular aggregates composed of human cells have better mechanical properties.

493  
494  
495  
496  
497  
498  
499  
500  
501  
502  
503  
504  
505  
506



**Fig. 9** Continuous bioprinting of live cells directly from computer models **a** *Rectangular* shaped **b** *Random-shaped* **c** *Zig-zag patterned circular* **d** *Spiral patterned circular* printed structures [83]

### 3 Conclusion and Discussion on Stem Cell Printing

Bioprinting is one of the most promising techniques in tissue engineering, where living cells are deposited layer-by-layer with or without biomaterials in user-defined patterns to build 3D tissue constructs. However, there are some challenges related with technical, material and cellular aspects. 3D bioprinting technology requires increased resolution, speed and compatibility with biologically relevant materials. Especially, the fabrication speed must be increased to create structures of clinically relevant sizes. Even the cells used for bioprinting applications are robust enough to survive the bioprinting process and withstand the physiological stresses; a large cell construct in an open environment may not survive a slow and therefore long printing process. For bioprinting, well-characterized and reproducible source of cells is required and any cell type selected for printing should be able to be proliferated into sufficient numbers for printing. Additionally, the proliferation

507 508  
 509  
 510 511  
 512  
 513  
 514  
 515  
 516  
 517  
 518  
 519  
 520  
 521  
 522  
 523  
 524  
 525

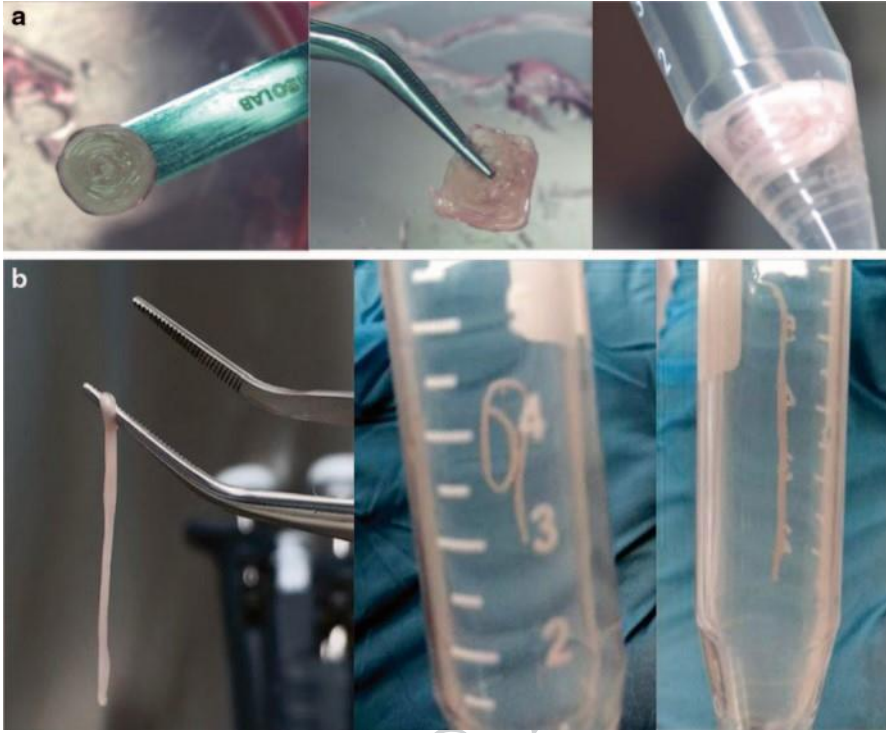


**Fig. 10** Bioprinted 3D totally biological tissue constructs without any biomaterial. **a** Circular and square shaped bioprinted with MOVAS, HUVEC and NIH 3T3 multicellular aggregates. **b** Stripe shaped bioprinted with HUVEC/HDF cell aggregates [83]

rate and the differentiation with small molecules or other factors should be controllable. Furthermore, sufficient vascularization and capillaries/microvessels are required for long-term viability of the fabricated construct and for tissue perfusion, respectively. The engineered structure should have suitable mechanical properties for physiological pressures and for surgical connection in case of transplantation. Bioreactors are used to maintain tissues *in vitro* and to provide maturation factors as well as physiological stressors for assembly, differentiation and ECM production prior to *in vivo* implantation.

Stem cells such as mesenchymal, induced pluripotent and embryonic stem cells could be a great source for bioprinting. Especially, printing differentiated or progenitor cells precisely and spatially could lead to multi-functional tissue constructs or even organs. However several challenges need to be overcome. First, bioprinting with stem cells requires large number of cells. Culturing this amount of stem cells could be really difficult. Especially, growing large number of stem cells on a feeder layer or special growth medium is really challenging. Even after culturing enough number of stem cells, bioprinting stem cells precisely and spatially accurate manner would require highly precise and special bioprinters. During bioprinting, the effect of compression on the viability and differentiation of stem cells should be considered. Since the stem cells are more susceptible to bioprinting conditions, more gentle and short printing procedures should be developed. Although the current 3D

528 bioprinting technology shows a great deal of promise to generate 3D layered con529  
 structs using live mixed cell populations, there is still a long way to go to create a 530  
 fully-functional organ.

531

532

533

## 534 References

535

536 1. Langer R, Vacanti JP. Tissue engineering. *Science*. 1993;260(0036-8075 (Print)):920–6.

537 2. Pollok JM, Vacanti JP. Tissue engineering. *Semin Pediatr Surg*. 1996;8:586(1055-8586  
 (Print)):191–6.

**AQ3** 38 3. Nakayama K. In vitro biofabrication of tissues and organs. In: Forgacs G, Sun W, editors. 539  
 Biofabrication: micro- and nano-fabrication, printing, patterning and assemblies. Elsevier;

540 2013. p. 1–16.

541 4. Atala A, Bauer SB, Soker S, Yoo JJ, Retik AB. Tissue-engineered autologous bladders for  
 542 patients needing cystoplasty. *Lancet*. 2006;367(9518):1241–6.

543 5. Brittberg M, Nilsson A, Lindahl A, Ohlsson C, Peterson L.. Rabbit articular cartilage defects  
 treated with autologous cultured chondrocytes. *Clin Orthop Relat Res*. 1996;326(0009-921X

544 (Print)):270–83.

545 6. Gallico GG, O'Connor NE, Compton CC, Kehinde O, Green H. Permanent coverage of large 546  
 burn wounds with autologous cultured human epithelium. *New Engl J Med*. 1984;311(7):448–

547 51.

548 7. Hibino N, McGillicuddy E, Matsumura G, Ichihara Y, Naito Y, Breuer C, et al. Late-  
 549 term results of tissue-engineered vascular grafts in humans. *J Thorac Cardiovasc Surg*.  
 2010;139(2):431–6.e2.

550 8. Matsumura G, Ishihara Y, Miyagawa-Tomita S, Ikada Y, Matsuda S, Kurosawa H,  
 Shin'oka 551 T, et al. Evaluation of tissue-engineered vascular autografts. *Tissue Eng*.  
 2006;12(1076-3279

552 (Print)):3075–83.

553 9. Niemeyer P, Krause U, Fellenberg J, Kasten P, Seckinger A, Ho AD, Simank HG, et al. Eval553  
 uation of mineralized collagen and alpha-tricalcium phosphate as scaffolds for tissue  
 engi554 neering of bone using human mesenchymal stem cells. *Cells Tissues Organs*. 2004;177(2)

555 (1422-6405 (Print)):880–5.

556 10. Oberpenning F, Meng J, Yoo JJ, Atala A. De novo reconstitution of a functional mammalian 557  
 urinary bladder by tissue engineering. *Nat Biotech*. 1999;17(2):149–55.

558 11. Radisic M, Park H, Shing H, Consi T, Schoen FJ, Langer R, et al. Functional assembly of 558  
 engineered myocardium by electrical stimulation of cardiac myocytes cultured on scaffolds.

559 *Proc Nati Acad Sci*. 2004;101(52):18129–34.

560 12. Shin'oka T, Matsumura G, Hibino N, Naito Y, Watanabe M, Konuma T, et al. Midterm  
 clini561 cal result of tissue-engineered vascular autografts seeded with autologous bone  
 marrow cells. 562 *J Thorac Cardiovasc Surg*. 2005;129(6):1330–8.

563 13. Nakamura M, Iwanaga S, Henmi C, Arai K, Nishiyama Y. Biomatrices and biomaterials for  
 563 future developments of bioprinting and biofabrication. *Biofabrication*. 2010;2(1):014110. 564 14. Wüst  
 S, Müller R, Hofmann S. Controlled positioning of cells in biomaterials—approaches 565 towards 3D tissue  
 printing. *J Funct Biomater*. 2011;2(3):119–54.

566 15. Melchels FPW, Domingos MAN, Klein TJ, Malda J, Bartolo PJ, Huttmacher DW. Additive 567  
 manufacturing of tissues and organs. *Prog Polym Sci*. 2012;37(8):1079–104.

568 16. Khoda AKM, Ozbolat IT, Koc B. A functionally gradient variational porosity architecture for

- 568 hollowed scaffolds fabrication. *Biofabrication*. 2011;3(3):034106.  
569
- 570 17. Khoda AKM, Ozbolat IT, Koc B. Designing heterogeneous porous tissue scaffolds for additive manufacturing processes. *Comput-Aided Des*. 2013;45(12):1507–23.
- 572 18. Matsuda N, Shimizu T, Yamato M, Okano T. Tissue engineering based on cell sheet technology. *Adv Mater*. 2007;19(20):3089–99.
- 573 19. Mironov V, Prestwich G, Forgacs G. Bioprinting living structures. *J Mater Chem*. 2007;17(20):2054–60.
- 575 20. Mironov V, Visconti RP, Kasyanov V, Forgacs G, Drake CJ, Markwald RR. Organ printing: tissue spheroids as building blocks. *Biomaterials*. 2009;30(12):2164–74.
- 577 21. Jakab K, Norotte C, Marga F, Murphy K, Vunjak-Novakovic G, Gabor F. Tissue engineering by self-assembly and bio-printing of living cells. *Biofabrication*. 2010;2(2):022001. 578
22. L'Heureux N, Dusserre N, Konig G, Victor B, Keire P, Wight TN, et al. Human tissue-engineered blood vessels for adult arterial revascularization. *Nat Med*. 2006;12(3):361–5.
- 580 23. L'Heureux N, Pâquet S, Labbé R, Germain L, Auger FA. A completely biological tissue-engineered human blood vessel. *FASEB J*. 1998;12(1):47–56.
- 581
24. Ferris C, Gilmore K, Wallace G, in het Panhuis M. *Biofabrication: an overview of the approaches used for printing of living cells*. *Appl Microbiol Biotechnol*. 2013;97(10):4243–58. 583
25. Marga F, Jakab K, Khatiwala C, Shepherd B, Dorfman S, Hubbard B, et al. *Toward engineering functional organ modules by additive manufacturing*. *Biofabrication*. 2012;4(2):022001. 584
26. Forgacs G, Foty RA, Shafir Y, Steinberg MS. *Viscoelastic properties of living embryonic tissues: a quantitative study*. *Biophys J*. 1998;74(5):2227–34. 585
- 586
27. Koç B, Hafezi F, Ozler SB, Kucukgul C. *Bioprinting-application of additive manufacturing in medicine*. In: Bandyopadhyay A, Bose S, editors. *Additive manufacturing*. CRC Press; in press. 588
- 589
28. Song S-J, Choi J, Park Y-D, Lee J-J, Hong SY, Sun K. *A three-dimensional bioprinting system for use with a hydrogel-based biomaterial and printing parameter characterization*. *Artif Organs*. 2010;34(11):1044–8. 590
- AQ6** 29. Chang CC, Boland ED, Williams SK, Hoying JB. *Direct-write bioprinting three-dimensional biohybrid systems for future regenerative therapies*. *J Biomed Mater Res B Appl Biomater*. 592  
2011;98B(1):160–70. 593
30. Odde DJ, Renn MJ. *Laser-guided direct writing for applications in biotechnology*. *Trends Biotechnol*. 1999;17(10):385–9. 594  
595
31. Nahmias Y, Schwartz RE, Verfaillie CM, Odde DJ. *Laser-guided direct writing for three-dimensional tissue engineering*. *Biotechnol Bioeng*. 2005;92(2):129–36. 596  
597
32. Zhen M, Russell KP, Qin W, Julie XY, Xiacong Y, Peng X, et al. *Laser-guidance-based cell deposition microscope for heterotypic single-cell micropatterning*. *Biofabrication*. 598  
2011;3(3):034107. 599
33. Murphy SV, Atala A. *3D bioprinting of tissues and organs*. *Nat Biotech*. 2014;32(8):773–85. 600
34. Guillotin B, Souquet A, Catros S, Duocastella M, Pippenger B, Bellance S, et al. *Laser-assisted bioprinting of engineered tissue with high cell density and microscale organization*. 601  
*Biomaterials*. 2010;31(28):7250–6. 602

- 603 35. Barron JA, Ringeisen BR, Kim H, Spargo BJ, Chrisey DB. Application of laser printing to 604 mammalian cells. *Thin Solid Films*. 2004;453–454(0):383–7.
- 605 36. Ringeisen BR, Kim H, Barron JA, Krizman DB, Chrisey DB, Jackman S, Auyeung RY, et al. Laser printing of pluripotent embryonal carcinoma cells. *Tissue Eng*. 2004;(1076–3279  
606 (Print))10(3–4):483–91.
- 607 37. Guillemot F, Souquet A, Catros S, Guillotin B, Lopez J, Faucon M, et al. High-throughput  
la608 ser printing of cells and biomaterials for tissue engineering. *Acta Biomater*. 2010;6(7):2494–  
609 500.
- 610 38. Haraguchi Y, Shimizu T, Yamato M, Okano T. Regenerative therapies using cell sheet-based tissue engineering for cardiac disease. *Cardiol Res Pract*. 2011;2011:845170.
- 611 39. Shimizu T, Yamato M, Isoi Y, Akutsu T, Setomaru T, Abe K, Kikuchi A, et al. Fabrication  
612 of pulsatile cardiac tissue grafts using a novel 3-dimensional cell sheet manipulation tech-  
613 nique and temperature-responsive cell culture surfaces. *Circul Res*. 2002;90(1524–4571  
(Electronic)):e40.
- 614 40. Imen Elloumi H, Masayuki Y, Teruo O. Cell sheet technology and cell patterning for  
615 biofab614 rication. *Biofabrication*. 2009;1(2):022002.
- 616 41. Shimizu T, Yamato M, Akutsu T, Shibata T, Isoi Y, Kikuchi A, et al. Electrically communi616 cating  
three-dimensional cardiac tissue mimic fabricated by layered cultured cardiomyocyte 617 sheets. *J Biomed  
Mater Res*. 2002;60(1):110–7.
- 618 42. Haraguchi Y, Shimizu T, Yamato M, Kikuchi A, Okano T. Electrical coupling of cardio-  
619 myocyte sheets occurs rapidly via functional gap junction formation. *Biomaterials*.  
2006;27(27):4765–74.
- 620 43. Shimizu T, Sekine H, Isoi Y, Yamato M, Kikuchi A, Okano T. Long-term survival and  
621 growth  
of pulsatile myocardial tissue grafts engineered by the layering of cardiomyocyte sheets.  
Tis622 sue Eng. 2006;12(1076–3279 (Print)):499–507.
- 623 44. Yamato M, Utsumi M, Kushida A, Konno C, Kikuchi A, Okano T.. Thermo-responsive cul-  
624 ture dishes allow the intact harvest of multilayered keratinocyte sheets without dispase by 624  
reducing temperature. *Tissue Eng*. 2001;7(1076–3279 (Print)):473–80.
- 625 45. Kushida A, Yamato M, Isoi Y, Kikuchi A, Okano T. A noninvasive transfer system for polar626 ized  
renal tubule epithelial cell sheets using temperature-responsive culture dishes. *Eur Cell 627 Materl*  
2005;10(1473–2262 (Electronic)):23–30.
- 628 46. Akizuki T, Oda S, Komaki M, Tsuchioka H, Kawakatsu N, Kikuchi A, et al. Application of  
629 periodontal ligament cell sheet for periodontal regeneration: a pilot study in beagle dogs. *J  
Periodontal Res*. 2005;40(3):245–51.
- 630 47. Hasegawa M, Yamato M, Kikuchi A, Okano T, Ishikawa I. Human periodontal  
631 ligament  
cell sheets can regenerate periodontal ligament tissue in an athymic  
rat model. *Tissue Eng*. 632 2005;11(1076–3279 (Print)):469–78.
- 633 48. Malda J, Visser J, Melchels FP, Jüngst T, Hennink WE, Dhert WJA, et al. 25th anniversary  
634 article: engineering hydrogels for biofabrication. *Adv Mater*. 2013;25(36):5011–28.
- 635 49. Nakamura M, Kobayashi A, Takagi F, Watanabe A, Hiruma Y, Ohuchi K, Iwasaki Y, et al.  
Biocompatible inkjet printing technique for designed seeding of individual living cells. *Tis636 sue  
Eng*. 2005;11(1076–3279 (Print)):1658–66.

- 637 50. Wilson WC, Boland T. Cell and organ printing 1: protein and cell printers. *Anat Rec A: Discov Mol, Cell, Evol Biol.* 2003;272 A(2):491–6.
- 638
51. Boland T, Mironov V, Gutowska A, Roth EA, Markwald RR. Cell and organ printing 2: fu639 sion of cell aggregates in three-dimensional gels. *Anatomical Rec A: Discov Mol, Cell, Evol Biol.* 2003;272 A(2):497–502.
- 641 52. Xu T, Jin J, Gregory C, Hickman JJ, Boland T. Inkjet printing of viable mammalian cells. *Biomaterials.* 2005;26(1):93–9.
- 642
53. Cui X, Boland T. Human microvasculature fabrication using thermal inkjet printing technol-  
643 ogy. *Biomaterials.* 2009;30(31):6221–7.
- 644 54. Boland T, Tao X, Damon BJ, Manley B, Kesari P, Jalota S, et al. Drop-on-demand  
645 printing of cells and materials for designer tissue constructs. *Mater Sci Eng: C.*  
2007;27(3):372–6.
- 646 55. Nakamura M, Nishiyama Y, Henmi C, Yamaguchi K, Mochizuki S, Koki T, et al. Inkjet  
647 bio-  
printing as an effective tool for tissue fabrication. *NIP Digital Fabr Conf.* 2006;2006(3):89–  
648 92.
56. Nishiyama Y, Nakamura M, Henmi C, Yamaguchi K, Mochizuki S, Nakagawa H, et al. De649 velopment of a three-dimensional bioprinter: construction of cell supporting structures using 650 hydrogel and state-of-the-art inkjet technology. *J Biomech Eng.* 2008;131(3):035001. 651 57. Xu C, Chai W, Huang Y, Markwald RR. Scaffold-free inkjet printing of three-dimensional 652 zigzag cellular tubes. *Biotechnol Bioeng.* 2012;109(12):3152–60.
58. Khatiwala C, Law R, Shepherd B, Dorfman S, Csete M. 3D cell bioprinting for regenerative  
653 medicine research and therapies. *Gene Ther Regul.* 2012;07(01):1230004.
- 654 59. Shabnam P, Madhuja G, Frédéric L, Karen CC. Effects of surfactant and gentle  
655 agitation on inkjet dispensing of living cells. *Biofabrication.* 2010;2(2):025003.
- 656 60. Chahal D, Ahmadi A, Cheung KC. Improving piezoelectric cell printing accuracy and  
657 reliability through neutral buoyancy of suspensions. *Biotechnol Bioeng.* 2012;109(11):2932–  
658 40.
61. Ferris CJ, Gilmore KJ, Beirne S, McCallum D, Wallace GG, In het Panhuis M. Bio-ink for  
659 on-demand printing of living cells. *Biomater Sci.* 2013;1(2):224–30.
- 658 62. Foty RA, Steinberg MS. The differential adhesion hypothesis: a direct  
659 evaluation. *Dev Biol.*  
2005;278(1):255–63.
- 660 63. Steinberg MS. Differential adhesion in morphogenesis: a modern view. *Curr Opin Genet*  
661 *Dev.* 2007;17(4):281–6.
64. Steinberg MS. Reconstruction of tissues by dissociated cells. Some morphogenetic tissue 662 movements and the sorting out of embryonic cells may have a common explanation. *Science.*  
663 1963;141(0036-8075 (Print)):401–8.
- 664 65. Jakab K, Norotte C, Damon B, Marga F, Neagu A, Besch-Williford CL, Kachurin A, et al. 665 Tissue engineering by self-assembly of cells printed into topologically defined  
666 structures. *Tissue Eng.* 2008;14(1937–3341 (Print)):413–21.
- 667 66. Kelm JM, Lorber V, Snedeker JG, Schmidt D, Broggini-Tenzer A, Weisstanner M, et al. A  
668 novel concept for scaffold-free vessel tissue engineering: Self-assembly of microtissue build-  
669 ing blocks. *J Biotechnol.* 2010;148(1):46–55.
- 670 67. Gwyther TA, Hu JZ, Christakis AG, Skorinko JK, Shaw SM, Billiar KL, et al. Engineered  
671 670 vascular tissue fabricated from aggregated smooth muscle cells. *Cells Tissues Organs.*  
2011;194(1):13–24.

68. Adebayo O, Hookway TA, Hu JZ, Billiar KL, Rolle MW. Self-assembled smooth muscle 672 cell tissue rings exhibit greater tensile strength than cell-seeded fibrin or collagen gel rings. *J*  
673 *Biomed Mater Res A*. 2013;101 A(2):428–37.
- 674 69. Napolitano AP, Chai P, Dean DM, Morgan JR. Dynamics of the self-assembly of complex  
675 cellular aggregates on micromolded nonadhesive hydrogels. *Tissue Eng*. 2007;13(1076–  
676 (Print)):2087–94.
- 677 70. Dean DM, Napolitano AP, Youssef J, Morgan JR, Rods, tori, and honeycombs: the di-  
678 rected self-assembly of microtissues with prescribed microscale geometries. *FASEB J*.  
2007;21(14):4005–12.
- 679 71. Khalil S, Nam J, Sun W. Multi-nozzle deposition for construction of 3D biopolymer tissue  
680 scaffolds. *Rapid Prototyp J*. 2005;11(1):9–17.
- 681 72. Khalil S, Sun W. Biopolymer deposition for freeform fabrication of hydrogel tissue constructs. *Mater*  
682 *Sci Eng: C*. 2007;27(3):469–78.
- 683 73. Smith CM, Christian JJ, Warren WL, Williams SK. Characterizing environmental factors that  
684 impact the viability of tissue-engineered constructs fabricated by a direct-write bioassembly tool.  
685 *Tissue Eng*. 2007;13(1076–3279 (Print)):373–83.
- 686 74. Smith CM, Stone AL, Parkhill RL, Stewart RI, Simpkins MW, Kachurin AM, Warren WL, 686 et al.  
687 Three-dimensional bioassembly tool for generating viable tissue-engineered constructs.  
*Tissue Eng*. 2004;10(1076–3279 (Print)):1566–76.
- 688 75. Duan B, Hockaday LA, Kang KH, Butcher JT. 3D Bioprinting of heterogeneous aortic valve  
689 conduits with alginate/gelatin hydrogels. *J Biomed Mater Res A*. 2012;101 A(5):1255–64.
- 690 76. Hockaday LA, Kang KH, Colangelo NW, Cheung PYC, Duan B, Malone E, et al. Rapid 690 3D  
691 printing of anatomically accurate and mechanically heterogeneous aortic valve hydrogel  
692 scaffolds. *Biofabrication*. 2012;4(3):035005.
- 693 77. Chang R, Nam J, Sun W. Effects of dispensing pressure and nozzle diameter on cell survival  
694 from solid freeform fabrication-based direct cell writing. *Tissue Eng*. 2008;14(1937–3341  
695 (Print)):41–8.
- 696 78. Cohen DL, Malone E, Lipson H, Bonassar LJ. Direct freeform fabrication of seeded  
697 hydrogels in arbitrary geometries. *Tissue Eng*. 2006;12(1076–3279 (Print)):1325–35.
- 698 79. Christopher MO, Françoise M, Gabor F, Cheryl MH. Biofabrication and testing of a fully cellular  
699 nerve graft. *Biofabrication*. 2013;5(4):045007.
- 700 80. Mironov V, Kasyanov V, Markwald RR. Organ printing: from bioprinter to organ  
701 biofabrication line. *Curr Opin Biotechnol*. 2011;22(5):667–73.
- 702 81. Norotte C, Marga FS, Niklason LE, Forgacs G. Scaffold-free vascular tissue engineering us700  
703 ing bioprinting. *Biomaterials*. 2009;30(30):5910–7.
- 704 82. Kucukgul C, Ozler SB, Inci I, Karakas E, Irmak S, Gozuacik D, et al. 3D bioprinting of 702 biomimetic  
aortic vascular constructs with self-supporting cells. *Biotechnol Bioeng*.  
2014;112(4):811–21 n/a-n/a.
83. Ozler SB, Kucukgul C, Koc B. 3D continuous cell bioprinting. submitted 2015.



UNCORRECTED PROOF

84. Kucukgul C, Ozler B, Karakas HE, Gozuacik D, Koc B. 3D hybrid bioprinting  
of macrovas<sup>705</sup>cular structures. *Procedia Eng.* 2013;59(0):183–92.